Crystal Structure of *n*-Paraffin Solid Solutions: An Electron Diffraction Study

Douglas L. Dorset

Electron Diffraction Department, Medical Foundation of Buffalo, Inc., Buffalo, New York 14203. *Received April 6, 1985*

ABSTRACT: Single-crystal electron diffraction data from epitaxially crystallized *n*-paraffins are used to characterize the structures of their solid solutions. The even–even binary chain system n-$C_{32}H_{66}/n$-$C_{36}H_{74}$ is shown to be continuous, preserving the orthorhombic polymorphic packing at all compositions. Intensity data ($0kl$) from a ca. 1:1 solid solution are used to verify the validity of a packing model similar to one proposed by Asbach et al. The continuity of the n-$C_{33}H_{68}/n$-$C_{36}H_{74}$ system is also demonstrated, contrary to predictions that these paraffins cannot form stable solid solutions because of dissimilar symmetry. It is shown, however, that epitaxial crystallization of the odd-chain paraffin produces a higher energy twinned monoclinic polymorphic form, which can more readily combine with the orthorhombic even-chain paraffin than can the lowest energy polymorph.

Introduction

Because the physical properties of numerous linear-chain molecular systems (e.g., polymers and acyl chain lipids) depend on the various chain lengths of components in a mixture, the thermal and crystallization behavior of mixed *n*-paraffin aggregates have often been studied.[1-7] A thermodynamic theory has been formulated for such mixed paraffin systems,[8] which basically states that the solid solution of two alkanes is favored if the Gibbs free energy of the mixed crystal is lower than those for the crystals of either pure component; otherwise there is no mixing in the solid state and a eutectic is formed.

The conditions for solid solution formation have also been stated in terms of molecular size and symmetry.[9,10] That is, if the component alkanes are too different in length, then the mixture is fractionated into the separate pure crystals upon cooling from the melt. In the case of paraffins with nearly the same chain length, molecular and crystal symmetry are most important. For example, as stated by Kitaigorodskii in his theory of solid solutions,[9] the insertion of molecule A into crystal B should not raise the symmetry of B and, indeed, should retain the symmetry of B if possible. Implicit in this argument, of course, is that molecule A and B are isomorphous so that no major lattice distortions are introduced when the components are mixed. In the case of *n*-paraffins this means that the symmetry of the total unit cell, including chain-end packing, in addition to the methylene subcell, is considered in an evaluation of miscibility.[10] Evaluations of earlier work on paraffin mixtures by Mnyukh[11] in terms of this theory apparently have detected systems where true solid solution is not allowed because of unfavored symmetry, despite the claims of the original workers.[3]

Although there is extensive treatment of the subject in earlier work, a number of questions remain yet in the description of solid solutions. For example, even though powder X-ray diffraction techniques are often used to characterize various crystalline forms, the overlap of diffraction peaks with nearly the same reciprocal spacing often masks subtle changes in crystal symmetry; indeed since the most intense reflections from paraffin crystals are due to the poly(methylene) sublattice, details of the total unit cell symmetry are further obscured. In fact, single crystals of paraffin solid solutions have not been characterized. The role of polymorphism, which may posit symmetries most favorable for continuous solid solution production, is very seldom mentioned. The role of point defects in such systems is also incompletely investigated.

Attempts to model the crystal structure of paraffin solid solutions[7] have shown that the major structural changes must occur at lamellar interfaces; i.e., there must be a disruption of the regular methyl-end plane packing found in pure paraffin crystals, which may or may not include point defects ("kinks") in the zigzag chain ends, in addition to possible longitudinal chain translations. Although Asbach and co-workers[7] favored a model for solid solutions (for which the shorter component concentration ≤70%) where the chains are mainly in the all trans conformation, interpretation of powder X-ray data again suffers the limitations mentioned above. Use of single-crystal diffraction data, on the other hand, would more readily detect any changes due to structural alteration of the methyl-plane interface and also, from the continuous diffuse scattering, identify the presence of possible chain defects. Thus, using electron diffraction techniques, which enable the description of microcrystals in terms of single-crystal diffraction intensities and symmetry, we report the respective solid solution crystal structures of even–even and odd–even paraffin chain mixtures, demonstrating why the latter solution is permitted. Included in these analyses is a demonstration of point defects, which may also modify the symmetry of component molecules.

Table I
Melting Point Data for Single Paraffins

compd	purity	onset	peak	lit.
n-dotriacontane (n-$C_{32}H_{66}$) (Eastman Chemical, Rochester, NY)	>95%	68.9	69.9	69.5–69.7[1]
n-tritriacontane (n-$C_{33}H_{68}$) (Fluka AG, Buchs, Switzerland)	>97%	71.0	72.1	71.8[14]
n-hexatriacontane (n-$C_{36}H_{74}$) (Aldrich Chemical, Milwaukee, WI)	98%	75.0	76.2	75.7–75.9[1]

Materials and Methods

***n*-Paraffins (Specimen Preparation).** Melting points of the three paraffins, which were measured with a Mettler FP800 DSC (see below), are listed in Table I. Although these samples are not extremely pure, their melting point values agree well with earlier reported values. Nevertheless, as shown by electron diffraction studies on solution crystallized material, the even-chain paraffins are of the orthorhombic polymorph described by Teare,[12] as also shown by our crystal-structure analysis of epitaxially crystallized specimens. The monoclinic polymorph[13] is never observed. The odd-chain paraffin also packs in the orthorhombic polymorph, but, as will be shown below, the epitaxially crystallized form is not the low-temperature structure described by Pieszczek et al.[14]

To prepare solid solutions of the paraffins, preweighed samples of the mixtures were fused. A small piece of the fused mass was then crushed in a mortar and pestle and the resultant powder

0024-9297/85/2218-2158$01.50/0

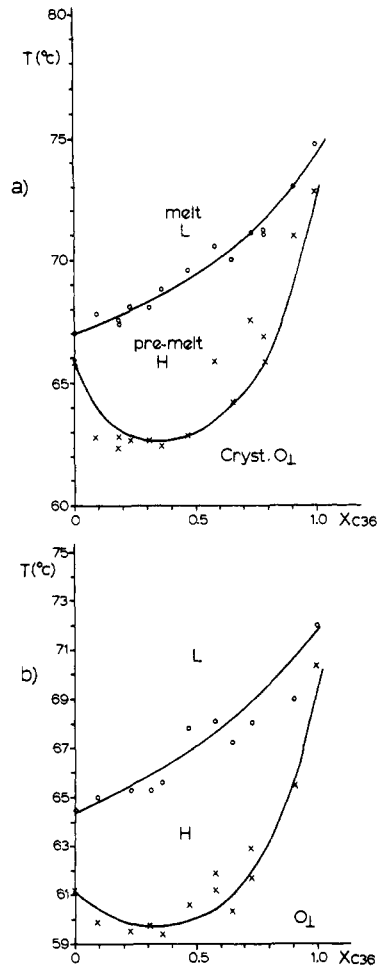

Figure 1. Melting (a) and freezing (b) curves for solid solutions of n-$C_{32}H_{66}$ with n-$C_{36}H_{74}$ as determined from DSC scans on prefused samples. The lower curves correspond to the orthorhombic-to-hexagonal solid-state transition while the upper ones denote the melt. Hysteresis in cooling vs. heating curves for pure components after correction of (b) for the instrumental lag mentioned above was noted also by Piper et al.[1] even though they claimed there was very little supercooling of the "setting point" on freezing in comparison to the melting point. An extensive treatment of hysteresis of solid-state transitions is given by Ubbelohde.[32]

spread on a freshly cleaved mica sheet. After a larger amount of benzoic acid was added, the other half of the mica plate was placed over the mixed sample to form a sandwich. Sliding this back and forth along a thermal gradient allows epitaxial crystal growth to occur, which is nucleated by the benzoic acid (procedure of Wittmann et al.[15]). The plates are then separated and covered with a thin carbon film, and the crystalline mass is then floated off onto a clean water surface to be picked up with electron microscope grids.

Electron Diffraction. All selected-area electron diffraction experiments were done at 100 kV with a JEOL JEM-100B electron microscope. Low beam dosages and a sensitive photographic emulsion (Kodak DEF-5 direct exposure film) ensured adequate protection of the specimens against radiation damage during the diffraction experiments. Calibration of camera lengths was made via an internal gold standard, after lightly coating representative specimens with a polycrystalline film in vacuo. Diffraction intensities were obtained by integration of scans with a Joyce Loebl MkIIIC flatbed microdensitometer.

Differential Scanning Calorimetry. Small pieces of the fused paraffin specimens were sealed in aluminum crucibles to be examined by differential scanning calorimetry using a Mettler FP800 apparatus at a scan rate of 2 °C/min. Typically a melting scan was followed by a cooling scan and then a further melting scan to measure both the melting and freezing points of the sample. In the representations below, the onset temperatures

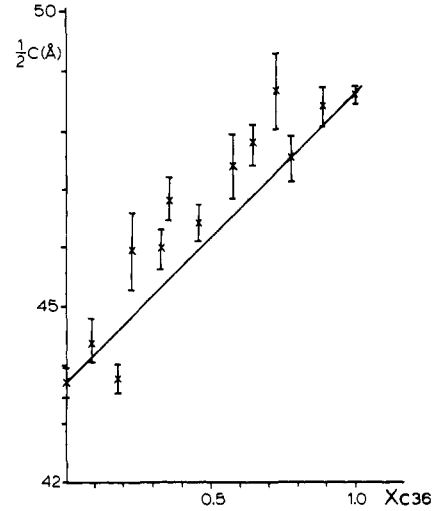

Figure 2. Experimentally measured electron diffraction lamellar spacings from epitaxially crystallized solid solutions of n-$C_{32}H_{66}$ with n-$C_{36}H_{74}$. For the pure paraffins, the measured spacings are respectively 43.69 ± 0.27 and 48.61 ± 0.16 Å compared to theoretical values[33] of 42.49 and 47.57 Å for the orthorhombic polymorph.[12]

of melting or freezing are used rather than the peak value. (To correct for instrument lag, 1.6° should be added to cooling curve values in data reported below.)

Calculations. Structure factors F_{hkl} were often calculated in the usual way

$$F_{hkl} = \sum_j f_j(\mathbf{s}_{hkl}) \exp(2\pi i \mathbf{r}\cdot\mathbf{s}_{hkl})$$

where the dot product

$$\mathbf{r}_j\cdot\mathbf{s}_{hkl} = h(x_j/a) + k(y_j/b) + l(z_j/c)$$

is sampled at integral values of the Miller indices (hkl). In other cases, i.e., for computations of diffuse continuous scatter or a mixed-component crystal, it was often useful to employ nonintegral Miller indices to probe scattering between Bragg peaks or to sample a continuous scattering function with reciprocal lattices having differing dimensions. In all cases, Doyle–Turner electron scattering factors[17] f_j were used for our computations. Although improved agreement of observed and calculated structure factors might be made via n-beam dynamical calculations,[18] these were not employed, owing to the complexity of the scattering model.

Even–Even Solid Solutions (n-$C_{32}H_{66}$ with n-$C_{36}H_{74}$)

The continuity of solid solutions of n-$C_{32}H_{66}$ with n-$C_{36}H_{74}$ is shown in the melting and freezing point curves of Figure 1, both for the orthorhombic-to-hexagonal phase transition and for the hexagonal-to-liquid melt.[19] Particularly for the pretransition, the plot is somewhat complicated by the presence of several onset temperatures for some mixtures, perhaps indicating several subtle changes in the crystal packing.[20]

Electron diffraction "long spacings" for the mixed-chain crystals are plotted in Figure 2. In all cases the appearance of the $0kl$ diffraction patterns completely resembles the single-crystal patterns from epitaxially nucleated crystals of pure paraffins published elsewhere[21] (Figure 3). The long spacings normally lie above the straight line joining the values for the pure components as also seen in X-ray determinations.[11] The deviations of these solid solution lamellar spacing measurements are somewhat larger than those of the pure component and, presumably, depict the local compositional variations in the solid expected as the sample is cooled from the liquidus to the solidus curve.[22] (Possibly this would be lessened on standing by solid-state diffusion[23,24].) Finally, it is inter-

Table II
Comparison of Observed 0*kl* Structure Factors from a ca. 1:1 Solid Solution of *n*-$C_{32}H_{66}$ with *n*-$C_{36}H_{74}$ to Calculated Values from Three Structure Models[a]

sample 4999			sample 5081				
hkl	$\|F_o\|$	$\|F_c\|(\sigma_1)$	*hkl*	$\|F_o\|$	$\|F_c\|(\sigma_1)$	$\|F_c\|(\sigma_2)$	$\|F_c\|(C_{34})$
002	0.51	0.51	002	0.67	0.74	0.78	0.31
004	0.46	0.40	004	0.55	0.63	0.60	0.31
006	0.39	0.41	006	0.37	0.48	0.38	0.30
008	0.27	0.38	008	0.27	0.34	0.21	0.30
0010	0.25	0.31	0068	0.27	0.12	0.11	0.20
0012	0.18	0.31	0070	0.86	1.21	1.27	1.29
0068	0.24	0.17	0072	0.83	0.90	0.84	1.00
0070	1.00	0.58	0074	0.21	0.16	0.15	0.19
0072	0.93	0.46	0130	0.25	0.12	0.10	0.17
0074	0.26	0.31	0132	0.42	0.23	0.22	0.25
0130	0.29	0.35	0134	0.81	0.70	0.72	0.64
0132	0.49	0.46	0136	1.57	1.17	1.22	1.29
0134	1.01	0.67	0138	0.37	0.08	0.08	0.17
0136	1.57	1.25	020	1.93	2.54	2.65	2.86
0138	0.40	0.41	022	0.44	0.25	0.27	0.25
020	1.88	2.39	024	0.41	0.24	0.24	0.15
022	0.32	0.56	026	0.38	0.18	0.11	0.08
024	0.36	0.38	0270	0.47	0.64	0.66	0.73
026	0.23	0.35	0272	0.51	0.52	0.54	0.58
0332	0.27	0.38	0332	0.37	0.24	0.23	0.26
0334	0.51	0.56	0334	0.60	0.89	0.93	0.85
0336	0.86	1.08	0336	1.17	1.34	1.40	1.55

[a] B_{iso} = 6.0 Å^2, only carbon atoms used in calculation. [b] For sample #4999, R = 0.27 ($|F_c|(\sigma_1)$] and for sample #5081, R = 0.29 ($|F_c/(\sigma_1)$), 0.31 ($|F_c|(\sigma_2)$), and 0.37 ($|F_c|(C_{34})$), where $R = [\sum||F_o| - k|F||/\sum|F_o|]$, scaled such that $\sum|F_o| = k\sum|F_c|$.

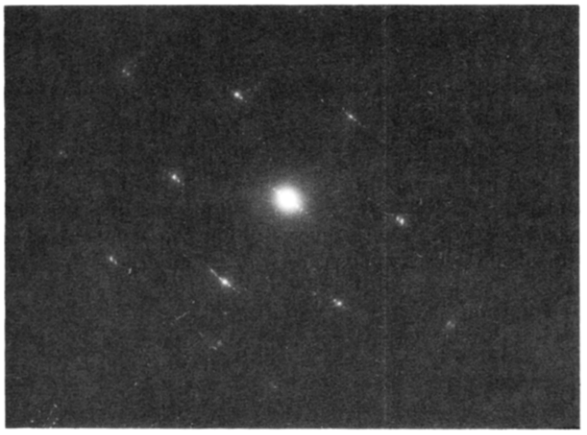

Figure 3. Electron diffraction pattern (0*kl*) from epitaxially crystallized solid solution (ca.1:1) of *n*-$C_{32}H_{66}$ and *n*-$C_{36}H_{74}$. Note the presence of diffuse scattering.

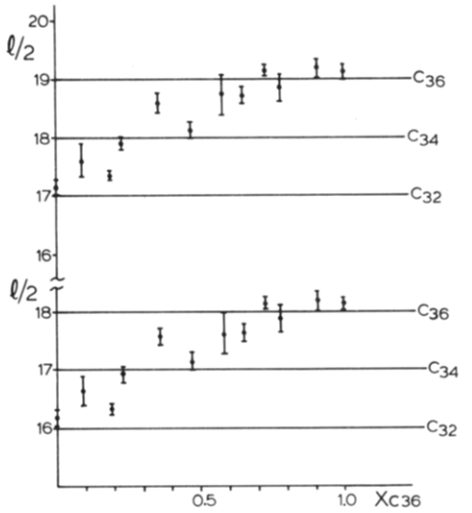

Figure 4. Index of two major 01*l* reflections from solid solutions of *n*-$C_{32}H_{66}$ with *n*-$C_{36}H_{74}$. (For the pure components these are the respective pairs [(0,1,32), (0,1,34)] and [(0,1,36), (0,1,38)]). Since the plotted values represent the c^* component of d^*_{01l} divided by d^*_{002}, the indicated l index is only half its actual value. As shown by an earlier crystal structure determination,[21] the symmetry is $Pca2_1$ and the structure agrees well with the orthorhombic form of *n*-hexatriacontane.[12] The prospect for other intermediate structures explaining Miller indices at e.g., x_{C36} = 0.09 has not been considered.

esting to plot the apparent indices of major 01*l* reflections for various solid solutions (Figure 4). Since a rather large reciprocal spacing is divided by a small value, some error is expected in this determination. However, it is shown that below x_{C36} = 0.1, the structure is basically that of the lower paraffin. Above this value and at least up to x_{C36} = 0.5, the mixed crystal behaves like $nC_{34}H_{80}$, as will be further demonstrated in the next section. At larger values of x_{C36} the crystals resemble the higher paraffin.

Crystal Structure of a 1:1 Solid Solution of *n*-$C_{32}H_{66}$ with *n*-$C_{36}H_{74}$

Similar to the analysis made by Asbach and co-workers[7] it was assumed that the major structural changes made in the orthorhombic paraffin structure by the production of solid solution are a Gaussian distribution of atom sites at the chain ends. Given a normalized Gaussian function

$$f(n) = (h/\pi^{1/2}) \exp(-h^2(n - m)^2)$$

where the standard deviation $\sigma = 1/(2^{1/2}h)$, two distributions were calculated by assuming σ = 14.03 and 28.05 (i.e., one or two methylenes) for the molecular weight of *n*-$C_{34}H_{70}$, m = 478.93, which is the mean molecular weight of a 1:1 solid solution of *n*-$C_{32}H_{66}$ with *n*-$C_{36}H_{74}$ considered here. Continuous Fourier transforms were calculated for orthorhombic paraffin structures at the resultant maximum lamellar lengths (respectively *n*-$C_{36}H_{74}$ and *n*-$C_{38}H_{78}$), weighing end atoms according to the calculated distributions, and these were subsequently sampled by the *n*-$C_{34}H_{70}$ reciprocal lattice to give the model structure factors. Observed structure factors are compared in Table II to these models and also structure factors calculated for pure orthorhombic *n*-$C_{34}H_{70}$. (The models are respectively designated σ_1, σ_2, C_{34}.) The resolution of lower angle 00*l*

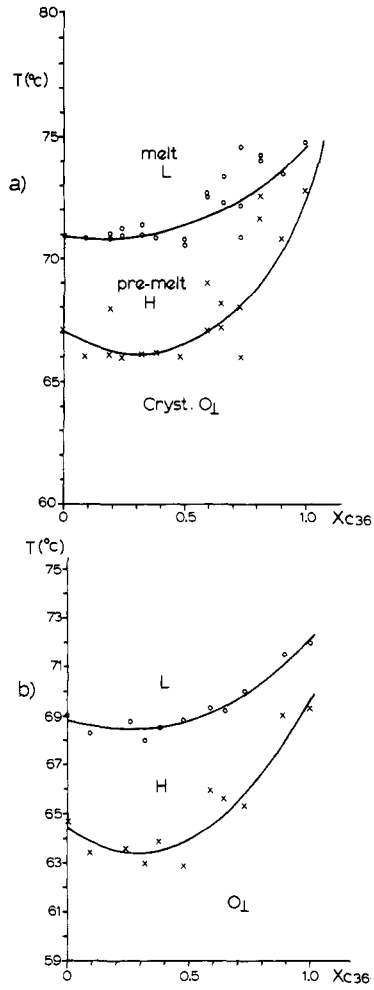

Figure 5. Melting (a) and freezing (b) point curves for the major transitions of the n-$C_{33}H_{68}$/n-$C_{36}H_{74}$ solid solutions. For some values of $x_{C36} > 0.5$, multiple crystal forms are indicated.

intensities in the latter model is only matched to the truncated range of these intensities often observed for solid solutions. The Gaussian model with narrowest distribution gives the best fit to experimental data and indicates that the longitudinal chain translation does not exceed the bounds set by the longest chain component.

Odd–Even Solid Solutions (n-$C_{33}H_{68}$ and n-$C_{36}H_{74}$)

The melting and freezing point curves (Figure 5) for the solid solutions of n-$C_{33}H_{68}$ with n-$C_{36}H_{74}$, like previous work with n-$C_{35}H_{72}$ and n-$C_{36}H_{74}$, also indicate continuity. A plot of long spacings for the mixed-component crystals (Figure 6) are again similar to the even–even solid solution plot above and those reported earlier for continuous solid solution based on X-ray diffraction measurements.[11] This facile solvation, which will be discussed in detail below, is apparent after a close scrutiny of the $0kl$ diffraction patterns from epitaxially crystallized pure n-$C_{33}H_{68}$. Indexing the major reflections and comparison to a structure factor calculation based on an alternative crystal packing[14] reveal that the crystal polymorph found here is not the low-temperature orthorhombic form originally described by Smith[25] but is actually the higher temperature twinned monoclinic form described by Piesczek et al.[14] (As will be reported elsewhere, this is confirmed by a quantitative crystal structure analysis from the measured intensity data.) A plot of reflection indices for major $01l$ peaks in the solid solution diffraction patterns (Figure 7) indicates that below $x_{C36} = 0.1$, the mixed crystals resemble n-$C_{33}H_{68}$. Beyond this point up to $x_{C36} = 0.32$, one finds a n-$C_{34}H_{70}$ type crystal, and at higher mole fractions of the higher alkane, the mixed crystals resemble n-$C_{36}H_{74}$.

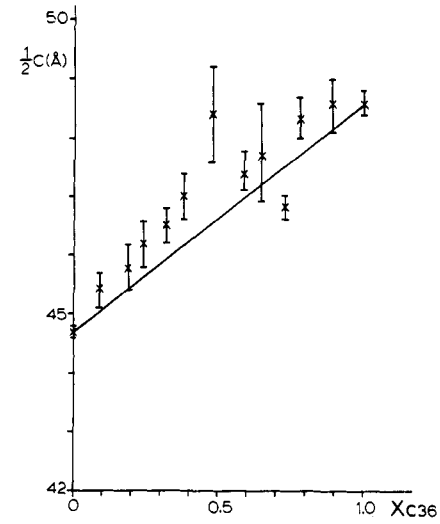

Figure 6. Electron diffraction lamellar spacings from epitaxially crystallized solid solutions of n-$C_{33}H_{68}$ with n-$C_{36}H_{74}$. The experimental lamellar spacing for n-$C_{33}H_{68}$ of 44.71 ± 0.12 Å is compared to a theoretical value of 43.89 Å for the low-temperature orthorhombic form[31] and measured values of 43.83 and 43.97 Å for respective orthorhombic and twinned monoclinic forms.[14]

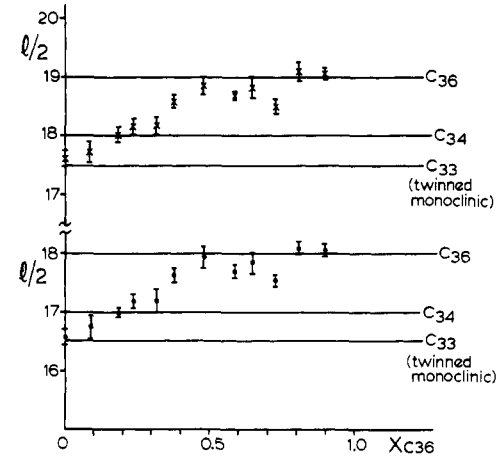

Figure 7. Indices of major $01l$ reflections for the n-$C_{33}H_{78}$/n-$C_{36}H_{74}$ solid solutions; again the plotted l value is half the actual, due to the zonal symmetry. (For pure n-$C_{33}H_{78}$, the major $01l$ reflections are (0,1,33) and 0,1,35).) The n-$C_{33}H_{78}$ pattern indicates that the structure is actually the twinned monoclinic form described by Piesczek et al.[14] with space group Aa and $a = 7.57$ Å, $b = 4.98$ Å, $c = 87.94$ Å, $\beta = 91.2°$. The cell dimensions of the orthorhombic n-$C_{36}H_{74}$ are[12] $a = 7.42$ Å, $b = 4.96$ Å, $c = 95.14$ Å.

Lattice Defects

In their X-ray analysis of the binary system n-$C_{28}H_{58}$ with n-$C_{32}H_{66}$, Asbach et al.[7] found that the best model for the crystal packing was one that allowed for longitudinal translations of the chains but did not include chain kinks at the ends. Because it was not possible to evaluate the background scatter adequately in the Debye–Scherrer patterns, these data could not be used as an independent assessment of this lattice distortion.

In our earlier electron diffraction studies on epitaxially crystallized paraffins,[26,27] the presence of kink defects was shown unequivocally, based in part on the salient directional diffuse scattering. Such continuous scatter is also clearly seen in diffraction patterns from epitaxially crystallized binary solid solutions (Figure 3). However, it is not possible to ascertain whether this defect concentration is any larger than for the single paraffin crystals, owing

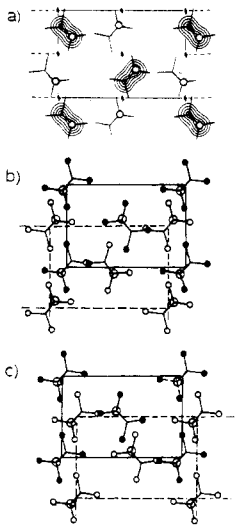

Figure 8. Comparison of the layer packing of (a) orthorhombic even-chain paraffins (data from Teare[12]) to the respective odd-chain paraffin packings of the (b) orthorhombic and (c) twinned monoclinic forms (data from Piesczek et al.[14]). In these figures the carbons bearing the third methyl hydrogen are circled. (The $a \simeq 7.5$ Å axis is horizontal and the $b \simeq 5.0$ Å axis is vertical). The correspondence of (a) and (c) is very close since methyl groups have the same polarity in chain rows parallel to b. In the orthorhombic odd-chain structure (b), on the other hand, this orientational polarity is parallel to a. Aside from having identical symmetry, the translations between chains in adjacent layers in the orthorhombic (even) case is $\Delta x = 0.78$ Å, $\Delta y = 2.48$ Å and in the twinned monoclinic (odd) case $\Delta x = 0.95$ Å, $\Delta y = 2.49$ Å. In the orthorhombic (odd) structure (b) the symmetry is changed and the respective chain center translations are $\Delta x = 1.16$ Å, $\Delta y = 2.48$ Å.

to the variations in crystal thickness; i.e., any increase in this diffuse intensity is not striking.

Discussion

The results obtained in this investigation of solid solutions may be used to modify the usual interpretation of Kitaigorodskii's theory;[9,10] i.e., when the likelihood of continuous solid solution formation was predicted from symmetry considerations, only the crystal packing of the lowest energy crystal polymorph was considered. In the case of the two even chain paraffins investigated here, both materials pack in the same series of polymorphs, beginning with the monoclinic structure described by Shearer and Vand[13] at lowest energy and progressing through the non-oblique orthorhombic form followed by the hexagonal premelt form. Even though the pure paraffins are monoclinic, the presence of slight impurities predisposes the orthorhombic form, as shown in recent X-ray studies.[7] In our case, the epitaxial nucleation produces orthorhombic symmetry for the pure species and this is continuously maintained for all solid solutions. DSC measurements also indicate that the single even-chain paraffins are in the orthorhombic form for the bulk samples. Nevertheless, solid solutions are allowed for every polymorphic modification.

The case of odd–even paraffin mixing is more interesting. Kitaigorodskii[10] and Mnyukh[11] criticized Mazee's[3] work on the n-$C_{35}H_{72}/n$-$C_{36}H_{74}$ system on the grounds that continuous solid solutions are not allowed by the divergent crystal symmetries in the pure components. However, as shown by Piesczek et al.,[14] there are various polymorphic forms of n-$C_{33}H_{68}$. Additionally, our data indicate that the epitaxially nucleated form is not the lowest energy polymorph. Thus to predict the likelihood of continuous solid solutions, one must examine the adaptability of this specific polymorph (which is very favorable) to the orthorhombic even-chain crystal structure. The twinned monoclinic (pseudoorthorhombic) polymorph of the odd-chain paraffin not only has the same subcell packing as the orthorhombic form with untilted chain axes (as is true for the lowest energy form), it most importantly has a very similar end-phase packing for contiguous layers as shown in Figure 8, giving a very close symmetry match. Likewise, of course, there are similar symmetries for the corresponding premelt hexagonal forms. In the bulk phase (examined via DSC), the lowest energy orthorhombic polymorph of the odd-chain paraffin would transform to the twinned monoclinic and again allow solid solution formation. However, even though such binary systems are stable for the higher temperature forms, they would not be stable for the lowest energy crystal packings for which the crystal symmetries are dissimilar. As also made clear from studies of "quasi-binary" polymer systems,[29] the existence of continuous solid solutions, therefore, may be possible for internal energy states that do not represent the true thermodynamic equilibrium of the system.[30] (This finding is supported also by the appearance of low-dose "lattice images" (McConnell, C., unpublished data) that demonstrate the continuity of these binary crystals.)

The single-crystal structure determination for a 1:1 solid solution is within the accuracy limits found for many electron diffraction analyses that lack corrections for dynamical scattering. Although this verification of a model similar to the one proposed by Asbach et al.[7] is very gratifying, no claims are made for its absolute accuracy. The major change in the diffraction pattern due to solid solution formation, aside from the shift of long spacing, is the attenuation of low-angle $00l$ reflections as noted by many workers before from X-ray data.[1,7] This change is very similar to the one produced by heating single crystals to near the premelt transition in that both events can be explained by enlarged end-plane void volumes.[7,28,26] Whether or not point defects ("kinks") have any increased role in solid solutions is difficult to say—even though this mechanism may be invoked to explain the partial filling of this void space (one can refer here to the crystal structures of cholesteryl esters determined at various temperatures, for which the major difference involves altered acyl chain end packing).[31] This point might be clarified in future work at low temperature, which hopefully will allow us to separate the thermal and disorder contributions to diffuse scattering from these binary crystals.

Acknowledgment. The author acknowledges the technical assistance of E. L. Hurley. Special thanks are due to Dr. A. Massalski for translations of several Russian articles. Research was supported by grants from the National Institutes of Health (GM21047) and the National Science Foundation (DMR 81-16318).

References and Notes

(1) Piper, S. N.; Chibnall, A. C.; Hopkins, S. J.; Pollard, A.; Smith, J. A. B.; Williams, E. F. *Biochem. J.* **1931**, *25*, 2072.
(2) Smith, J. C. *J. Chem. Soc.* **1932**, 737.
(3) Mazee, W. M. *Anal. Chim. Acta* **1957**, *17*, 97.
(4) Nechitailo, N. A.; Rozenberg, L. M.; Terent'eva, E. M.; Topchiev, A. V. *Dokl. Akad. Nauk SSSR* **1957**, *116*, 613.
(5) Nechitailo, N. A.; Topchiev, A. V.; Rozenberg, L. M.; Terent'eva, E. M. *Russ. J. Phys. Chem. (Engl. Transl.)* **1960**, *34*, 1268.
(6) Kitaigorodskii, A. I.; Mnyukh, Yu, V.; Nechitailo, N. A. *Sov. Phys. (Eng. Transl.) Crystallogr.* **1958**, *3*, 303.
(7) Asbach, G. I.; Geiger, K.; Wilke, W. *Colloid Polym. Sci.* **1979**, *257*, 1049.
(8) Asbach, G. I.; Kilian, H. G. *Ber. Bunsen-Ges. Phys. Chem.* **1970**, *75*, 814.

(9) Kitaigorodskii, A. I. "Organic Chemical Crystallography"; Consultant's Bureau: New York, 1961; p 231.
(10) Kitaigorodskii, A. I. "Molecular Crystals and Molecules"; Academic Press: New York, 1973; p 116.
(11) Mnyukh, Yu. V. *Zh. Strukt. Khim* **1960**, *1*, 370.
(12) Teare, P. W. *Acta Crystallogr.* **1959**, *12*, 294.
(13) Shearer, H. M. M.; Vand, V. *Acta Crystallogr.* **1956**, *9*, 379.
(14) Piesczek, W.; Strobl, G. R.; Malzahn, K. *Acta Crystallogr. Sect. B: Struct. Crystallogr. Cryst. Chem.* **1974**, *B30*, 1278.
(15) Wittmann, J. C.; Hodge, A. M.; Lotz, B. *J. Polym. Sci., Polym. Phys. Ed.* **1983**, *21*, 2495.
(16) Amoros, J. L.; Amoros, M. "Molecular Crystals. Their Transforms and Diffuse Scattering"; Wiley: New York, 1968.
(17) Doyle, P. A.; Turner, P. S. *Acta Crystallogr. Sect. A: Cryst. Phys., Diffr., Gen. Crystallogr.* **1968**, *A24*, 390.
(18) Cowley, J. M. "Diffraction Physics", 2nd ed.; North Holland: Amsterdam, 1981; p 238ff.
(19) Müller, A. *Proc. R. Soc. London, A* **1932**, *138*, 514.
(20) Maroncelli, M.; Qi, S. P.; Strauss, H. L.; Synder, R. G. *J. Am. Chem. Soc.* **1982**, *104*, 6237.
(21) Moss, B.; Dorset, D. L.; Wittmann, J. C.; Lotz, B. *J. Polym. Sci., Polym. Phys. Ed.* **1984**, *22*, 1919.
(22) Azaroff, L. V. "Introduction to Solids"; McGraw-Hill: New York, 1960; pp 186ff.
(23) Ungar, G.; Keller, A. *Colloid Polym. Sci.* **1979**, *257*, 90.
(24) Zerbi, G.; Piazza, R.; Holland-Moritz, K. *Polymer* **1982**, *23*, 1921.
(25) Smith, A. E. *J. Chem. Phys.* **1953**, *21*, 2229.
(26) Dorset, D. L.; Moss, B.; Wittmann, J. C.; Lotz, B. *Proc. Natl. Acad. Sci. U.S.A.* **1984**, *81*, 1913.
(27) Dorset, D. L.; Moss, B.; Zemlin, F. *J. Macromol. Sci. Phys.*, in press.
(28) Strobl, G.; Ewen, B.; Fischer, E. W.; Piesczek, W. *J. Chem. Phys.* **1974**, *61*, 5257.
(29) Smith, P.; Manley, R. St. J. *Macromolecules* **1979**, *12*, 483.
(30) Wunderlich, B. "Macromolecular Physics, Crystal Melting"; Academic Press: New York, 1980; Vol. 3, p 83ff.
(31) Sawzik, P. Ph.D. Thesis, University of Pittsburgh, Pittsburgh, PA, 1984.
(32) Ubbelohde, A. R. "The Molten State of Matter"; Wiley: New York, 1978; Chapter 4.
(33) Nyburg, S. C.; Potoworowski, J. A. *Acta Crystallogr., Sect. B: Struct. Crystallogr. Cryst. Chem.* **1973**, *B29*, 347.

Influence of the Head-to-Head Defect and the Molecular Weight on the $\alpha \rightarrow \gamma$ Solid-State Transformation of Poly(vinylidene fluoride)

Lien Tai Chen and Curtis W. Frank*

Department of Chemical Engineering, Stanford University, Stanford, California 94305.
Received June 4, 1984

ABSTRACT: Crystallization of PVF_2 from the melt results in three peaks in the melting endotherm obtained by differential scanning calorimetry; these correspond to α, crystallized γ, and transformed γ forms. An additional low-melting peak is attributed to the interlamellar crystallization that occurs during quenching. Areas of these peaks are determined and used to study the solid-state $\alpha \rightarrow \gamma$ transformation. The extent of the transformation appears to increase with the percentage of the γ spherulites in the crystalline regions but to decrease with the content of the interlamellar amorphous layers. The results support Lovinger's proposal that the transformation proceeds more rapidly in the longitudinal direction toward the α-nuclei than in the transverse direction. Moreover, the two competing factors—the percentage of the γ spherulites and the interlamellar amorphous content—increase with either the reversed monomer (head-to-head defect) content or the molecular weight. As a result, the $\alpha \rightarrow \gamma$ transformation is a complex function of the head-to-head defect concentration and the molecular weight.

Introduction

Poly(vinylidene fluoride) (PVF_2) has been extensively studied and much is known about the morphological and electrical characteristics.[1] The focus of this work is on the α and γ polymorphs that are formed upon crystallization from the melt.[2] In particular, we wish to examine the influence of the reversed monomer content, or head-to-head (H/H) defect, and the molecular weight on the solid-state $\alpha \rightarrow \gamma$ transformation. This transformation is of interest because the α form, containing two molecular chains of TGTG′ conformation in the unit cell, is nonpolar, whereas the γ form, containing two chains of TTTGTTTG′ conformation, is polar. Thus, high-temperature annealing could potentially be used to transform a piezoelectrically inactive sample into a piezoelectrically active one.

Prest and Luca[3] were the first to report on the $\alpha \rightarrow \gamma$ solid-state transformation in a study employing differential scanning calorimetry and infrared spectroscopy. Proposals for the molecular mechanism have been made by Takahashi and Tadokoro[4] and by Lovinger.[5] In addition, Lovinger[6] has also suggested a bulk mechanism involving the morphological superstructure. A major objective of this paper is to provide quantitative verification of Lovinger's[6] proposal through application of differential scanning calorimetry to well-characterized commercial samples of PVF_2.

Table I
Area Ratios from Differential Scanning Calorimetry Melting Endotherms Used in the Correlations in Figures 2–7

sample	H/H defect content	mol wt	$A_p/(A_\alpha+A_{\gamma'})$	$A_{\gamma'}/(A_\alpha+A_{\gamma'})$	$A_{\gamma'}/(A_\alpha+A_\gamma+A_{\gamma'})$
SU 53	3.3	140 000	0.0	1.9	2.6
SU 51	3.6	130 000	0.0	2.1	0.8
Solvay 537	4.0	52 000	0.0	1.2	2.1
Solef 1012	4.0	222 000	9.4	0.0	1.8
Dyflor 2000E	4.2	135 000	2.4	2.4	2.1
Solef 1008	4.2	101 000	6.2	5.6	5.6
Solvay 671	4.4	703 000	22.5	5.4	12.8
Solef 1010	4.5	146 000	7.1	5.2	4.8
Dyflor 2000L	5.1	94 000	14.3	2.1	4.7
Kynar 880	5.3	186 000	25.7	2.9	4.8
Dyflor 2000H	5.3	207 000	24.7	9.7	22.5

0024-9297/85/2218-2163$01.50/0